Performance Evaluation of IREDA prototype system: an IR-based Portable Electronic Detection System for Blood Alcohol Concentration

Panayiota Demosthenous[1], Kleanthis Erotokritou[1] and Marios Sergidis[1]
[1] *Cy.R.I.C. Cyprus Research & Innovation Center Ltd, 28th October st, Nicosia, Cyprus*
{p.demosthenous, k.erotokritou, m.sergidis}@cyric.eu

Keywords: Ethanol Detection; Blood Alcohol Concentration (BAC); Breath Alcohol Concentration (BrAC); Transdermal Alcohol Concentration (TrAC); Tissue Alcohol Concentration (TAC) Near Infrared (NIR), Diffused Reflectance, Tissue Phantoms, Integrating Sphere, Touch-based Detection, Gas-based Detection.

Abstract: This paper demonstrates a prototype system called IREDA, which is an IR-based Portable Electronic Detection System for Blood Alcohol Concentration. IREDA examines, a) the fusibility on detecting Ethanol on human body via NIR diffused reflectance with a touch-based oriented detection, and b) the fusibility on detecting Ethanol in human respiration via multiple light absorptions with gas-based detection. IREDA has proved the fusibility on detecting Ethanol vapour with LOD of about 12mg/L, and the fusibility on detecting Ethanol in solid gelatine samples. However, it was difficult for now to compare these results with data involving real human tissue and alcohol consumption.

1 INTRODUCTION

Driving under the influence (DUI) of alcohol is responsible for the 25% of all road fatalities in European Union. According to European Commission Communication, efficient means to control alcohol intake and advice users on their ability to drive are critical to prevent accidents. The need to monitor indirectly the blood alcohol level of people for safety, medical, legal or health reasons, as well as, for safe recreational alcohol consumption, leaded to several non-invasive solutions that use biofluids samples such as, tears, saliva, sweat, or measure either the breath alcohol concentration (BrAC) or the tissue alcohol concentration (TAC).

Breathalyzers are widely used for determining BAC indirectly [1], but their resulting measurements usually suffer from inaccuracies due to interference from external and internal factors such as humidity, temperature, individuals' traits, subject physiological variations, contamination of mouth compounds and environmental vapours. Two other methods, an eyeglasses-based tear biosensing device [2] and a saliva electrochemical ring sensor [3], use biofluids samples. However, the first involves tears stimulation and the second is missing pH & temperature sensors for compensating temperature changes or variations in the saliva pH. Moreover, there are several other transdermal alcohol sensing methods [4] that detect either the liquid or gas phase of alcohol just above the skin. However, detection in generated sweat can only be achieved if sweat is produced after a stimulation process, which in general introduces limitations. Furthermore, individual, and environmental factors (e.g., skin thickness, gender differences, humidity, temperature), are introducing variations in transdermal alcohol readings, which also present late response with a time lag of a couple of hours. Last but not least, non-invasive optical methods exist for blood alcohol concentration measurements on tissue sample, among which, infrared spectroscopy (IR) was found to be the most promising, employing either near-infrared spectrum [5] or mid-infrared spectrum [6]. Specifically, wavelength-modulated differential photothermal radiometry (WM-DPTR), has the capability of measuring BAC with high resolution at around 5mg/dl and low detection limit at around 10mg/dl. However, this methodology is currently using laboratory equipment, presenting limitations on further miniaturization for personal use.

This paper demonstrates a prototype system called IREDA, which is an IR-based Portable Electronic Detection System for Blood Alcohol

Concentration. IREDA examines, a) the fusibility on detecting Ethanol on human body via NIR diffused reflectance with a touch-based oriented detection [7], and b) the fusibility on detecting Ethanol in human respiration via multiple light absorptions with gas-based detection [8].

The system uses as a main optical part, an integrating sphere for the efficient collection of the diffused light from the sample in the case of touch-based detection. Integration spheres are known to be beneficial in some spectroscopic applications [9] and are used to enhance the collection of backscattered light in non-invasive sensing applications such as, finger photo plethysmography for determine blood concentration [10], and laser spectroscopy for glucose sensing [11]. To examine near infrared (NIR) diffused reflectance on simulating tissues, the experiments use, low-cost optical tissue phantoms [12] composing of water, gelatine, and titanium dioxide (TiO_2) powder. Such samples are commonly used in optical applications to simulate human tissue. Likewise, integrating spheres are beneficial in gas sensing applications, as they easily increase the effective optical path length from the light source to the detector. Hence, the interaction length between light and gas sample becomes higher [13], increasing the sensitivity of a gas-based detection system.

The following sections present the system implementation, as well as the experimental testing & results for the performance evaluation of IREDA.

2 SYSTEM IMPLEMENTATION

This section describes; a) the hardware architecture of the system, b) the optical setup and optoelectronics that has been used, c) the system's software with the signal processing algorithm, and finally d) the overall system integration.

2.1 System's Hardware Architecture

There are several individual modules that are included in the hardware development of IREDA. These are a) the current driver & b) the temperature controller of the light sources, c) the transimpedance amplifier of the photodetector, and d) the main control unit (MCU) of the system. Figure 1, shows the architecture of the hardware electronic subsystem. This design presents all the connections between the specified peripherals and clarifies the communication protocols and the digital and analog signals between them, as well as the power supply requirements.

A laser diode driver FL500 by Wavelength electronics (FL591FL), has been chosen to drive the NIR light sources at a constant current mode. This module can drive two independent outputs up to 250mA, controlled by two separate modulation signals. A temperature controller PTC5K-CH by Wavelength electronics, has been chosen to set and control the temperature of the light sources, ensuring wavelength stability during the optical measurements. A transimpedance amplifier AMP100 by Thorlabs was chosen, for the amplification of the photodetector signal. This amplifier converts photodiode's output current to voltage with a switchable gain from 1, 10 and 100 MV/A. An sbRIO-9627 controller from National Instruments has been used as the MCU. The MCU is responsible to control all the above peripherals, the laser driver, the TECs and the photodetector. Specifically, the MCU is responsible to; a) Set the optical intensity and wavelength of the NIR light sources, b) Read the photodetector signal, and c) Provide the collected data to the 'data analysis software'.

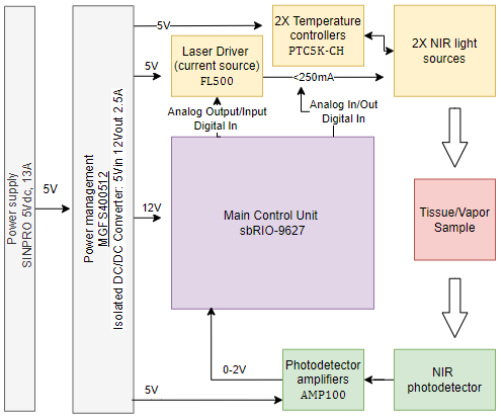

Figure 1: The hardware architecture of IREDA.

The optical intensity can be controlled with the laser driver (FL591FL) that applies a constant or pulse current through the lasers' anode and cathode. The wavelength of the laser can be control be changing the lasers' temperature using the temperature controller (PTC5K-CH). While the light sources illuminate the sample, the photodetector collects the reflected radiation that gives the information of Ethanol existence within the sample. The radiation produces a photocurrent to the photodiode, which needs amplification via the transimpedance amp (AMP100) that consecutively converts the current to a readable voltage. This voltage is then digitized by an ADC on the MCU (sbRIO-9627). The raw data of the optical measurement are then provided to the Labview-based data analysis software for further processing.

2.2 Optics and Optoelectronics

The optical setup described in this section is designed to accommodate two separate infrared light sources, which can be detected by a single photodetector. The schematic of the optical setup used for IREDA, is show in Figure 2.

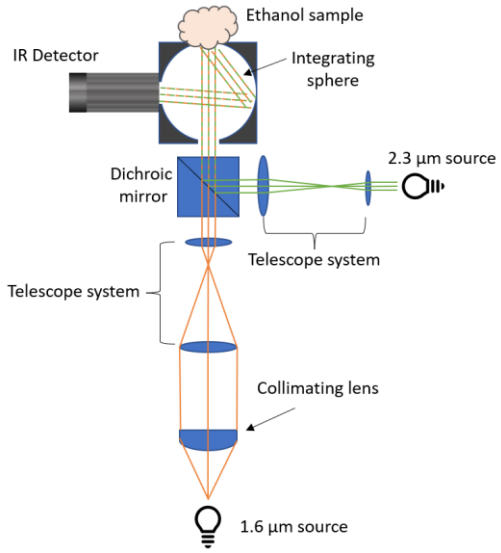

Figure 2: Schematic of the optical apparatus.

This spectroscopic setup consists of two IR sources at 1.6 µm and 2.3 µm. The former is an LED (Roithner LaserTechnik, LED16) connected to a temperature-controlled mount (Thorlabs, LDM56). The 2.3 µm source is a distributed feedback laser diode (Sacher Lasertechnik, DFB-2274-002-TO66). Directly after the 1.6 µm LED source, a plano-convex lens (Thorlabs, LA1951) is used as a collimator. Subsequently, the collimated beam passes through an inversed telescope system formed by two additional lenses to reduce the beam diameter down to slightly less than 8 mm which is the port opening of the integrating sphere. The two lenses used are f = 1000 mm (Thorlabs, LB1409) and f = 50 mm (Thorlabs, LB1471) respectively and placed at 1050 mm distance between them. In the path of the 2.3 µm source merely a telescope system is advised, consisting of 15 mm and 35 mm focal length lenses to increase the beam diameter in this case. The two beams then arrive at a short pass dichroic mirror with cut-off wavelength at 1800 nm (Thorlabs, DMSP 1800R) allowing for wavelengths shorter than 1800 nm to be transmitted and longer wavelengths to be reflected. The combined beams then enter the integrating sphere (Thorlabs, 2P4) and strike the sample (i.e. finger) which is placed at the opposite port. An integrated sphere is chosen here to collect the light that is diffusely reflected by the sample at all angles, thus maximizing the detector's signal and increasing signal stability. As mentioned previously, the beam diameter from both light sources is reduced to be slightly smaller than the port diameter of the integrating sphere. This is done to allow the light to only interact with a maximum area of the sample without being directly reflected by the inner walls of the sphere. An IR detector (Thorlabs, FD10D) is connected to the side port to measure light intensity as reflected by the sample. The fine adjustment of the lens systems was achieved by leaving the top port of the sphere open in the absence of sample. Since both beams are collimated and with diameters slightly less than port size, the detected signal was almost null. The maximum device signal was detected when the top port was closed with the reflective-coated plug.

The actual optical setup is shown in Figure 3. This optical setup, as has been described above, can be used as a touch-based detection system for Ethanol detection in 'tissue' samples. At the same time, this setup can be used as a gas-based detection system for vapor Ethanol detection, where the multiple reflections of the light within the integrating sphere offer multiple absorption paths into the gas that fulfils the sphere. The deference in that case is that the top port of the sphere is kept closed with its reflective-coated plug, while the side port of the sphere now serves as the gas/vapor inlet port.

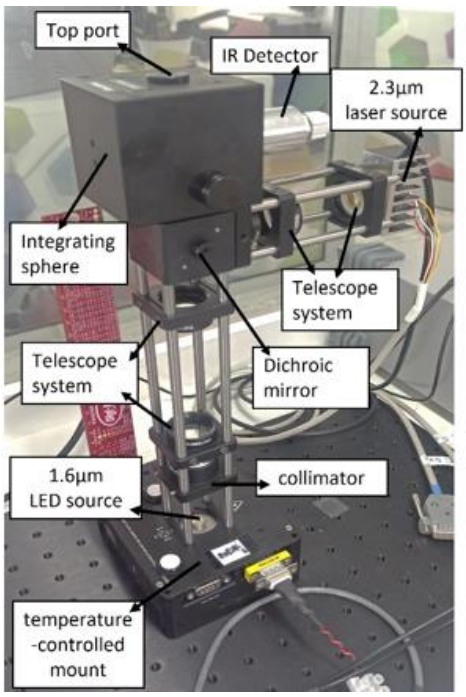

Figure 3: The optical setup of IREDA.

2.3 System Software-Signal Processing

During an optical measurement, both light sources (LSs) are operated simultaneously and are pulsed with a rectangular waveform with a duty cycle of 50%. While LS2 is modulated with a frequency, LS1 is modulated with the double frequency (Figure 4). Then, a synchronous detection of the photodetector (PD) signal is done digitally by sampling the measurement and modulation signals (Sync. Signal 1/2) and processing them via the data analysis software of IREDA. Figure 4 shows an example of the two synchronization signals and the PD measurement signal, where the PD signal is a superposition of both excitation signals.

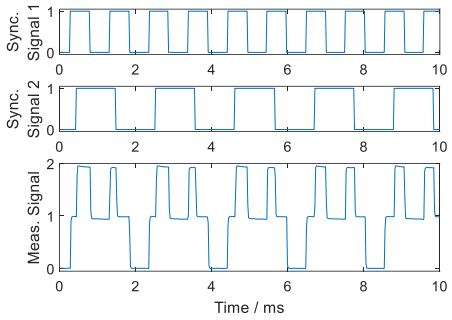

Figure 4: Measured signals from the photodetector

Figure 5 sketches the digitally implemented lock-in signal processing algorithm. With a rectangular excitation signal being used for both LSs, the algorithm is basically a multiplication of the measurement signal with the sign of the mean value free synchronization signal [14].

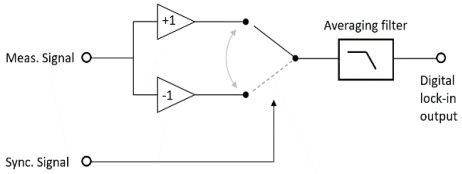

Figure 5: Principle of the digital synchronous detector.

Figure 6 shows the software of IREDA, where the results are visualized in real time. The temperature control of the light sources (LSs) can be accessed from the left lower corner square, while their current control and modulation can be accessed from the left upper corner square. The modulation signals of the two LSs can be visualized and verified in the 'Current Measurement' window, where you can also observe the PD measurement signal. In the 'Real Time Results' window the three plots correspond, to LS1 response, to LS2 response, and to the Ratio LS1/LS2. As can be seen in Figure 6, by removing the side port of the integrating sphere, both LSs record a signal decrease, resulting from the light escaping the sphere and never detected by the photodetector.

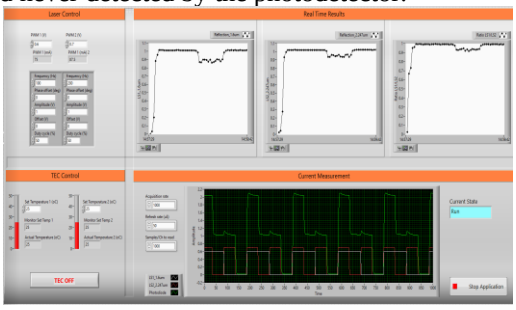

Figure 6: Final IREDA software.

2.4 System Integration

The optical setup, the electronic hardware, and the data analysis software were integrated together within an acrylic enclosure to construct IREDA system. Figure 7 and Figure 8 present the final integrated prototype system, indicating the main modules and optical components.

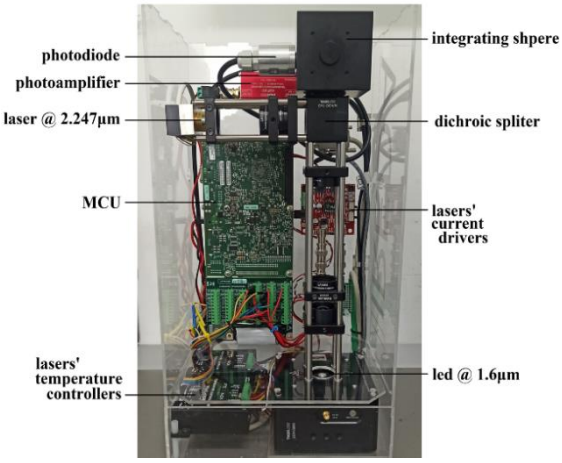

Figure 7: The integrated IREDA prototype.

3 EXPERIMENTAL TESTING AND RESULTS

This section describes the experimental testing for the performance validation of IREDA, both as a) a touch-based and b) gas-based Ethanol-detection system. Both experiments use the same configuration parameters. Therefore, the voltage applied to the 1.6μm LED source was set at 1V, and 1.5V for the 2.3μm laser source, while the two sources were modulated at 0.1kHz and 0.2kHz respectively (Figure 8). The photo amplifier connected to the photodiode detector was set to an amplification of 10 MV/A.

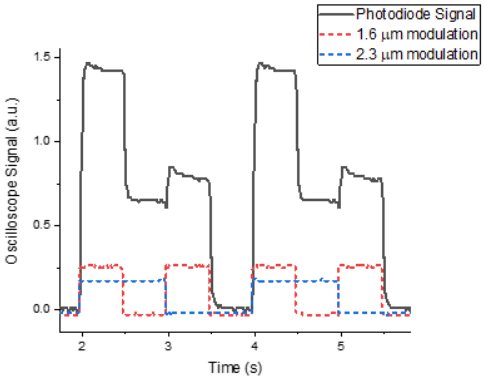

Figure 8: Example of the modulation and photodiode signals as measured via the oscilloscope signal.

3.1 Validation of the Gas-based Detection System

3.1.1 Experimental configuration using latex balloon as the vapour provider

A latex balloon was used to provide the integrating sphere with a constant volume of ethanol vapour. A specific amount of liquid solution was added to the rubber balloon prior inflation. The balloon was then inflated to a constant volume and sealed allowing the liquid to evaporate for several seconds. The balloon was then connected to the "sample port" via a tube (Figure 11) and the air-vapour mixture was released into the sphere. Due to the constant volume of air used in this method, an actual sample concentration can be calculated by approximating the balloon volume to that of a sphere.

Data collection initiated prior connecting the balloon to the sample port to ensure zero absorption i.e., maximum PD signal. The balloon was then allowed to deflate resulting to PD signal drop due to absorption. Afterwards the balloon was disconnected. An additional balloon with different ethanol concentration was connected after observing maximum PD signal denoting "empty" sphere. Figure 9 shows an example of a raw data sequence recorded in this set of experiments. Different regions represent time periods where the integrating sphere contained no ethanol vapour (empty), was filled with vapour (filling) and finally exhausting the vapour again (emptying).

Different concentrations of ethanol were investigated with this configuration, ranging from 15 – 240 mg/L. It was observed that indeed increasing ethanol concentration resulted to a greater drop in PD signal for 2.27 μm, with a maximum decrease of 10% recorded for the highest concentration. In the case of the 1.6 μm light source the change in absorption is less significant. Figure 10 presents the normalised PD signal for the time that maximum absorption was observed for both light sources used.

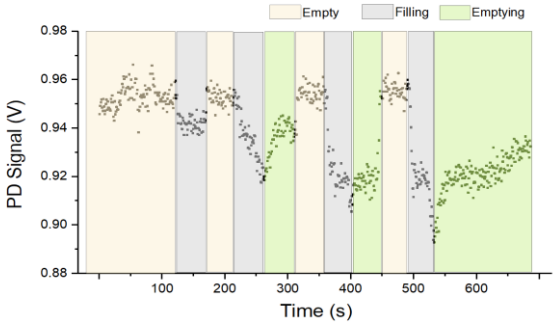

Figure 9: Example of photodiode signal. The different coloured time regions represent the process of ethanol vapour entering and exiting the integrating sphere.

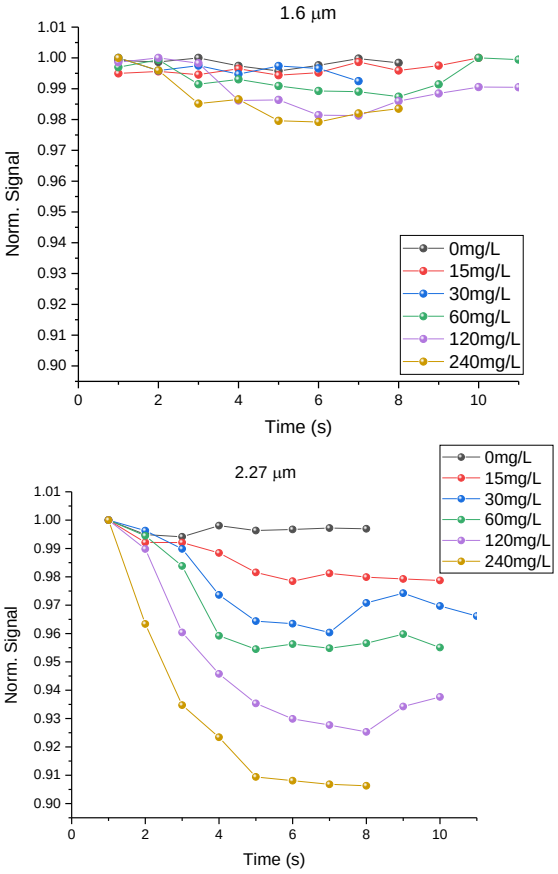

Figure 10: Normalised photodiode signal for (a) 1.6 μm and (b) 2.27 μm light sources, for different concentrations of ethanol vapour. Data presented here are up to the time where minimum PD signal was observed i.e., maximum absorption.

As a results, the collected data confirmed the capability of detecting alcohol vapour, while making it was possible to differentiate between different concentrations. As a next step, lower concentrations of alcohol vapor needed to be evaluated to assess the limit of detection, as well as to compare to a commercial device.

3.1.2 Experimental configuration using a commercial Breathalyser

In order to compare the detection of gas ethanol in IREDA to a commercial device, a breathalyser was incorporated to the experimental setup. Additionally, the concentration calculation method could be verified by this process. A split Y-tube was connected to the sample port so that the vapour from the latex balloon entered the breathalyser and the integrating sphere at the same time. An image of the modified experimental setup is shown in Figure 11.

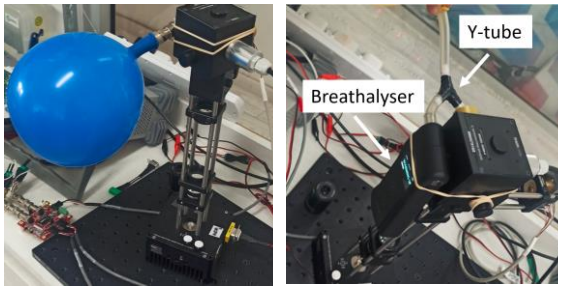

Figure 11: Air-filled balloon connected to the setup (left), Modified experimental setup with a breathalyser (right).

Initially, different amount of liquid ethanol was inserted into the latex balloon prion inflating it. The balloon was then inflated to a diameter of approximately 20±1cm and connected to the Y-tube. Upon deflation the reading of the breathalyser and PD signal were recorded. It was noted that the breathalyser was saturated at about 14 μL of added liquid ethanol. A linear relation between the amount of ethanol added and the breathalyser reading was observed as shown in Figure 12. By fitting the data, a conversion factor from μL to mg/L of 0.172 mg/L/μL was obtained, which was in agreement with the one derived by the concentration calculations for a 21cm diameter sphere and 90% ethanol (0.171 mg/L/μL). It is noteworthy that the PD signal was indistinguishable for these lower concentration values (Figure 13). The minimum concentration that the apparatus was able to detect was 12 mg/L of ethanol vapour. Furthermore, the signal for 1.6μm presented relatively minor changes for different concentrations and for this reason the data is omitted here. It can be concluded that the IREDA setup in its present form has an alcohol vapour detection limit of about 12 mg/L which is in the range of the upper limit of some commercial breathalysers.

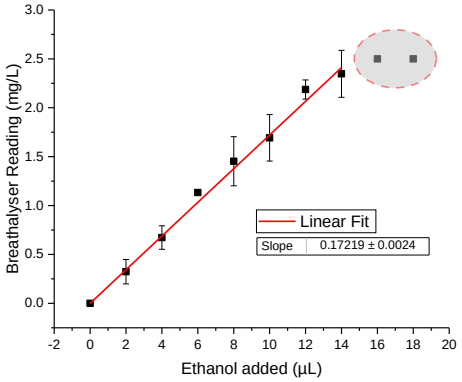

Figure 12: Breathalyser reading versus volume of ethanol added to the latex balloon. The breathalyser saturated for values over 14 μL. The red solid line represents the linear fit of the data giving a conversion factor of 0.172 mg/L/μL.

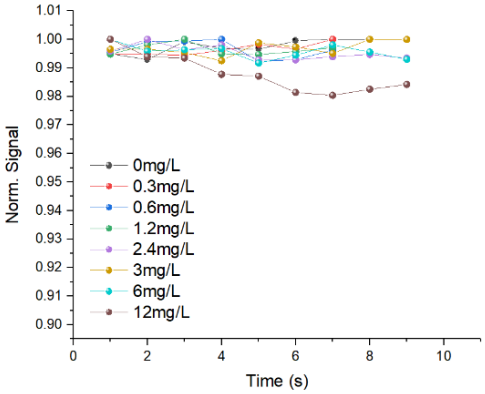

Figure 13: Normalised PD signal of the 2.27μm laser source for lower ethanol concentrations between 0 and 12 mg/L. No notable change in signal was observed for concentrations below 12 mg/L.

3.1.3 Experimental configuration using an air-pressure regulator valve

To further optimize the setup, a pressure regulator was added between the balloon and the integrating sphere. This offered a controlled flow of gas mixture and granted monitoring light absorption as the integrating sphere was slowly filled. The regulator was set at a constant pressure of 0.2 bar. This eliminated the problem of the ethanol vapour mixture entering and exiting the sphere rapidly thus creating inconsistencies in the measurements. As the sample vapour was flowing into the sphere, the photodiode signal was decreased, eventually reaching a minimum value. As the sphere was filled with ambient air, absorption decreased, resulting to increased photodiode signal.

The experiments were again divided into two concentration groups, low and high. The first one ranged from 0 – 7.5 mg/L with an additional high concentration of 30 mg/L for testing purposes, while the second group consisted of higher concentrations ranging from 0 – 120 mg/L. Figure 14 presents the normalised signal at 2.27μm for both groups. Similarly to the previous measurements a noticeable drop in PD signal for high concentrations was observed but not in the case of the lower values. Nevertheless, the incorporation the regulator to the setup allowed for the collection of a greater number of data points during each run which also revealed fluctuations in the signal over time.

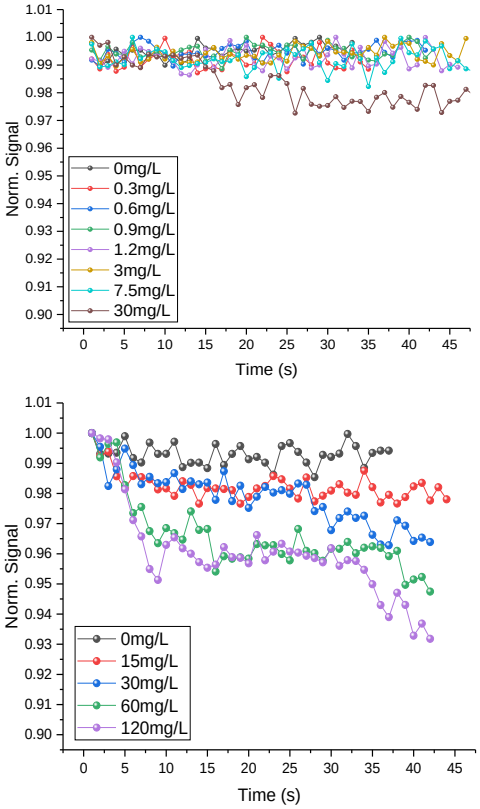

Figure 14: Normalised PD signal of the 2.27 μm laser source for (left) lower and higher (right) ethanol concentrations while the ethanol vapour flow was controlled by a pressure regulator set at 0.2 bar.

Afterwards, the repeatability of data collection was assessed for a longer period. For these measurements, a latex balloon was filled with a certain amount of ethanol and deflated through the regular. The integrating sphere was then "cleaned" with fresh air and then filled again with the same concentration of ethanol vapour. This was repeated three time for each concentration value. A plot of the average signal versus concentration revealed a linear relationship (Figure 15), which in turn gave the rate of signal decrease with concentration, and it was found to be -0.0013 (mg/L)-1 which can be considered as the sensitivity of the device.

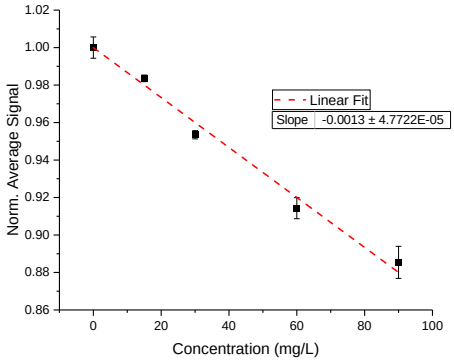

Figure 15: Average of the minimum signal versus ethanol concentration. The dashed red line is the linear fit of data.

3.2 Touch-based Detection System Validation with gelatine samples

Subsequently, alcohol vapour was replaced by a gelatine mixture to test the device operation with solid samples resembling human tissue. Gelatine was the best candidate since it possesses similar properties with human tissue, it is easily accessible and cheap. The samples were prepared by mixing gelatine powder with water and TiO2. The mixture was shaken for 5 minutes, microwaved for 20 seconds, and rotated on a carousel for 20 minutes. Then, it was placed in shallower round plastic containers (volume = 2.5 ml) as shown in
Figure 16.

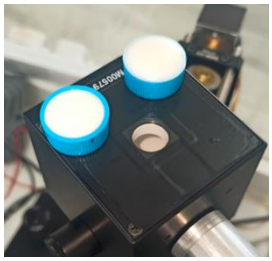

Figure 16: Gelatine sample in shallow plastic containers.

The sample was placed at the top port so the incoming light from the sources was directly incident on the gelatine while a known amount of ethanol was injected via syringe. Data were collected on individual samples by increasing the injected ethanol after a period. At some point the sample was allowed to relax so the ethanol was completely evaporated as shown in Figure 17. This was done to test that the

signal returns to maximum (no absorption) while using the same sample in the absence of ethanol. The results revealed that by increasing the injected amount of ethanol in gelatine the 2.27μm photodiode signal further decreased. Even though, it is difficult to compare these results with data involving real human tissue and alcohol consumption, it is evident that the IREDA setup can detect changes in ethanol concentration present in solid samples.

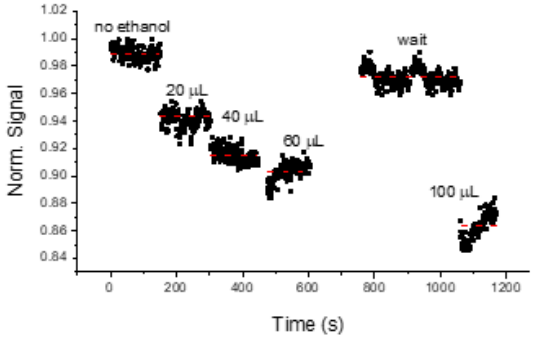

Figure 17 : Normalised PD signal of the 2.27 μm laser source for added injected ethanol volume in gelatine samples. Dashed red lines represent the average values.

4 CONCLUSIONS

IREDA has proved the fusibility on detecting Ethanol vapour that simulate human respiration, via multiple light absorptions within an integrating sphere, leading to a gas-based detection setup with LOD of about 12mg/L. Moreover, the fusibility on detecting Ethanol in solid gelatine samples that simulate 'tissue' samples, via touch-based oriented detection and NIR diffused reflectance has been proved. Although, it is difficult to compare these results with data involving real human tissue and alcohol consumption.

ACKNOWLEDGEMENTS

The work was supported by the Project POST-DOC/0718/0186 which is co-financed by the European Regional Development Fund and the Republic of Cyprus through the Research and Innovation Foundation.

REFERENCES

[1] Jurič, A.; Fijačko, A.; Bakulić, L.; Orešić, T.; Gmajnički, I. Evaluation of breath alcohol analysers by comparison of breath and blood alcohol concentrations. *Archives of Industrial Hygiene and Toxicology* **2018**, *69*, 69-76.

[2] Sempionatto, J.R.; Brazaca, L.C.; García-Carmona, L.; Bolat, G.; Campbell, A.S.; Martin, A.; Tang, G.; Shah, R.; Mishra, R.K.; Kim, J. Eyeglasses-based tear biosensing system: Non-invasive detection of alcohol, vitamins and glucose. *Biosensors and Bioelectronics* **2019**,*137*,161-170.

[3] Mishra, R.K.; Sempionatto, J.R.; Li, Z.; Brown, C.; Galdino, N.M.; Shah, R.; Liu, S.; Hubble, L.J.; Bagot, K.; Tapert, S. Simultaneous detection of salivary Δ9-tetrahydrocannabinol and alcohol using a Wearable Electrochemical Ring Sensor. *Talanta* **2020**, *211*, 120757.

[4] Fairbairn, C.E.; Kang, D. Temporal Dynamics of Transdermal Alcohol Concentration Measured via New‐Generation Wrist‐Worn Biosensor. *Alcoholism: Clinical and Experimental Research* **2019**, *43*, 2060-2069.

[5] Ver Steeg, B.; Treese, D.; Adelante, R.; Kraintz, A.; Laaksonen, B.; Ridder, T.; Legge, M.; Koslowski, N.; Zeller, S.; Hildebrandt, L. Development of a Solid State, Non-Invasive, Human Touch Based Blood Alcohol Sensor. In Proceedings of 25th International Technical Conference on the Enhanced Safety of Vehicles (ESV) National Highway Traffic Safety Administration.

[6] Guo, X.; Shojaei-Asanjan, K.; Zhang, D.; Sivagurunathan, K.; Sun, Q.; Song, P.; Mandelis, A.; Chen, B.; Goledzinowski, M.; Zhou, Q. Highly sensitive and specific noninvasive in-vivo alcohol detection using wavelength-modulated differential photothermal radiometry. *Biomedical Optics Express* **2018**, *9*, 4638-4648.

[7] P. Demosthenous and M. Baer, Near Infrared Diffused Reflectance on Tissue Simulating Phantoms for Optical Applications, in Proceedings of OPAL 2022 - 5th International Conference on Optics, Photonics and Lasers, 18-20 May 2022, pp.12-14.

[8] P. Demosthenous and M. Baer, Infrared Spectroscopic Application using an Integrating Sphere for Measuring Vapor Ethanol, in Proceedings of OPAL 2022 - 5th International Conference on Optics, Photonics and Lasers, 18-20 May 2022, pp.15-17.

[9] LM. Hanssen, KA. Snail, Handbook of Vibrational Spectroscopy: Integrating spheres for mid-and near-infrared reflection spectroscopy, John Wiley & Sons, 2002.

[10] T. Yamakoshi, J. Lee, K. Matsumura, Y. Yamakoshi, P. Rolfe, D. Kiyohara, KI. Yamakoshi, Integrating sphere finger-photoplethysmography: preliminary investigation towards practical non-invasive measurement of blood constituents, PloS one, Vol. 10, Issue 12, 2015, p.e0143506.

[11] A. Werth, S. Liakat, A. Dong, CM. Woods, CF. Gmachl, Implementation of an integrating sphere for the enhancement of noninvasive glucose detection using quantum cascade laser spectroscopy, Applied Physics B, Vol. 124, Issue 5, 2018, pp. 1-7.

[12] L. Ntombela, B. Adeleye, N. Chetty, Low-cost fabrication of optical tissue phantoms for use in biomedical imaging, Heliyon, Vol. 6, Issue 3, 2020, p.e03602.

[13] S. Tranchart, IH. Bachir, JL. Destombes, Sensitive trace gas detection with near-infrared laser diodes and an integrating sphere, Applied optics, Vol. 35, Issue 36, 1996, pp. 7070-7074.

[14] M. Baer, B. Schmauss, P. Demosthenous, Simultaneous Signal Acquisition by Synchronous Detection of Orthogonal Frequency Components, in Proceedings of

SMSI 2021 Conference - Sensor and Measurement Science International, 3-6 May 2021, pp. 254-255.